Osteoarthritis and Cartilage (2009) **17,** 1029–1039

doi:10.1016/j.joca.2009.02.009

Osteoarthritis and Cartilage

International Cartilage Repair Society

OARSI OSTEOARTHRITIS RESEARCH SOCIETY INTERNATIONAL

Composition-function relationships during IL-1-induced cartilage degradation and recovery

A. W. Palmer†§, C. G. Wilson‡§, E. J. Baum‡§ and M. E. Levenston†§*

† *George W. Woodruff School of Mechanical Engineering, Georgia Institute of Technology, Atlanta, GA 30332, United States*

‡ *Wallace H. Coulter Department of Biomedical Engineering, Georgia Institute of Technology, Atlanta, GA 30332, United States*

§ *Parker H. Petit Institute for Bioengineering and Bioscience, Atlanta, GA 30332, United States*

Summary

Objective: To examine the relationships between biochemical composition and mechanical properties of articular cartilage explants during interleukin-1 (IL-1)-induced degradation and post-exposure recovery.

Design: Bovine articular cartilage explants were cultured for up to 32 days with or without 20 ng/mL IL-1. The dynamic shear modulus $|G^*_{dyn}|$ and equilibrium and dynamic unconfined compression moduli (E_{equil} and $|E^*_{dyn}|$) were measured at intervals throughout the culture period. In a subsequent recovery study, explants were cultured for 4 days with or without 20 ng/mL IL-1 and for an additional 16 days in control media. The dynamic moduli $|E^*_{dyn}|$ and $|G^*_{dyn}|$ were measured at intervals during degeneration and recovery. Conditioned media and explant digests were assayed for sulfated glycosaminoglycans (sGAG) and collagen content.

Results: Continuous IL-1 stimulation triggered progressive decreases in E_{equil}, $|E^*_{dyn}|$, and $|G^*_{dyn}|$ concomitant with the sequential release of sGAG and collagen from the explants. Brief IL-1 exposure resulted in a short release of sGAG but not collagen, followed by a gradual and incomplete repopulation of sGAG. The temporary sGAG depletion was associated with decreases in both $|E^*_{dyn}|$ and $|G^*_{dyn}|$ which also recovered after removal of IL-1. During IL-1-induced degradation and post-exposure recovery, explant mechanical properties correlated well with tissue sGAG concentration.

Conclusions: As previously shown for developing cartilages and engineered cartilage constructs, cytokine-induced changes in sGAG concentration (i.e., fixed charge density) are coincident with changes in compressive and shear properties of articular cartilage. Further, recovery of cartilage mechanical properties can be achieved by relief from proinflammatory stimuli and subsequent restoration of tissue sGAG concentration.

Key words: Interleukin-1, Cartilage degradation, Cartilage mechanics, Composition-function relationships.

Introduction

Articular cartilage is comprised of chondrocytes embedded within an extracellular matrix (ECM) consisting primarily of the large, aggregating proteoglycan (PG) aggrecan, type II collagen, and water. The high density of negatively charged sulfated glycosaminoglycans (sGAG) attached to the aggrecan core protein gives rise to an osmotic swelling pressure that resists compression and is balanced by tensile stresses carried by the collagen fiber network. Due to low tissue permeability, dynamic physiologic loads are carried primarily through pressurization of entrapped fluid[1]. The resident chondrocytes synthesize and remodel the ECM[2–5] but can also contribute to tissue destruction in various degenerative conditions.

Quantitative relationships between ECM molecule content and cartilage mechanical properties have been explored through regression analyses in healthy, developing, and degenerating articular cartilage[6–13]. These studies demonstrated statistically significant correlations between the concentration of sGAG and the compressive stiffness, and elevated sGAG concentrations were inversely correlated with the hydraulic permeability. The collagen concentration was also well-correlated with cartilage properties, indicating that the mechanical function of cartilage hinges on contributions from PGs and collagen. In addition, the interaction of PGs and the collagen network under cyclic and steady-state loads has been extensively characterized by the dynamic and equilibrium moduli in compression, shear and tension[17–20]. There are no reports, however, of composition-function regression analyses for cartilage undergoing cytokine-induced degradation.

Interleukin-1 (IL-1) cytokines have demonstrated roles in promoting cartilage matrix resorption *in vitro* and mediating inflammation *in vivo*. Within hours of exposure to exogenous IL-1, chondrocytes in monolayer and explants upregulate and activate aggrecanases, leading to proteolysis and release of PGs[3–25]. Following PG release, the collagen network undergoes MMP-mediated degradation[14,24–26]. Furthermore, IL-1 decreases sGAG[14,27–29] and protein

*Address correspondence and reprint requests to: Marc E. Levenston, Stanford University, Department of Mechanical Engineering, 233 Durand Building, Stanford, CA 94305-4038, United States. Tel: 1-650-723-9464; Fax: 1-650-725-1587; E-mail: levenston@stanford.edu

Received 26 March 2008; revision accepted 16 February 2009.

synthesis[14,30–32]. IL-1-induced depletion of PGs and collagen degradation are accompanied by increases in permeability and decreases in equilibrium and dynamic compressive moduli and compression-induced streaming potential[14,24]. Autocrine IL-1 expression is believed to play a role in cartilage matrix remodeling as part of homeostasis[33], and chondrocytes have been reported to restore PG content and PG synthesis following transient IL-1 exposure *in vitro* and *in vivo*[25,34–37]. However, the extent to which this PG repopulation restores the mechanical properties of recovering cartilage has not been examined.

The studies described here present detailed time courses of the biochemical and biophysical changes associated with IL-1-induced cartilage degradation. The loss and subsequent recovery of matrix constituents in response to transient IL-1 exposure are also described, along with detailed measurements of the physical properties of these recovering explants. Based on linear regression analysis, the relationships between cartilage composition and mechanical properties in both the degrading and recovering explants are described. The results of these experiments, which further illuminate the roles of PGs and collagen in cartilage mechanics during tissue degradation and recovery, lend insight into targets for diagnosis and treatment.

Methods

TISSUE EXPLANT PREPARATION AND CULTURE

Under aseptic conditions, 3 mm diameter full thickness cartilage explants were harvested with a biopsy punch (Miltex, York, PA) from the femoral condyles and patellar grooves of both stifles of an immature calf (Research 87, Boylston, MA). A custom cutting block was used to remove the most superficial ~300 μm and the deep zone tissue, resulting in middle zone explants with a thickness of 1.78 ± 0.020 mm as measured with digital calipers. Forty explants were randomly assigned to either control or IL-1-stimulated groups. To allow for equilibration to culture conditions, explants were precultured for 72 h at 37°C and 5% CO_2 in serum-free control medium consisting of high glucose Dulbecco's Modified Eagle's Medium (DMEM) supplemented with 50 μg/mL gentamicin, 0.1 mM non-essential amino acids (Invitrogen, Carlsbad, CA) and 50 μg/mL ascorbate (Sigma, St. Louis, MO). Explants were placed two per well in 48 well plates (Becton Dickinson, Franklin Lakes, NJ) in 0.5 mL of either control medium or control medium supplemented with 20 ng/mL recombinant human IL-1α (Peprotech, Rocky Hill, NJ). This IL-1 dosage has been shown to induce aggressive cell-mediated degradation, with complete depletion of sGAGs within 2 weeks[24,38]. Samples were cultured for up to 32 additional days, with media changed and collected every 48 h. Four explants per group were removed from culture at days 4, 8, 12, 16, 24, and 32 and stored in 0.15 M Dulbecco' phosphate buffered saline (DPBS) (Invitrogen) with protease inhibitors (PI Cocktail Set I, Calbiochem, San Diego, CA) at −20°C for subsequent compression testing and biochemical analysis.

A second degradation study was conducted specifically to examine changes in shear properties due to IL-1 stimulation. Sixty-five explants (4 mm diameter × 2 mm thick) were isolated as described above from middle zone cartilage of a second calf. Following a 3-day preculture, explants were cultured in individual wells for up to 24 additional days in 0.5 mL of control medium or control medium supplemented with 20 ng/mL IL-1α. Five explants per group were removed from culture at days 0, 4, 8, 12, 16, 20, and 24 and stored in 0.15 M DPBS with protease inhibitors at −20°C for subsequent dynamic shear testing and biochemical analysis.

To study recovery from transient IL-1 exposure, 36 explants (4 mm diameter × 2 mm thick) were isolated as described above from middle zone cartilage of a third calf. Following a 3-day preculture, the explants were cultured for 4 days in 0.5 mL of either control medium or control medium supplemented with 20 ng/mL IL-1α, followed by up to 16 days of culture in control medium. Four explants per group were removed at days 0, 4, 8, 12 and 20 and stored in 0.15 M DPBS with protease inhibitors at −20°C for subsequent mechanical testing and biochemical analysis.

To examine whether IL-1 exposure decreased cell viability, explants (4 mm diameter × 2 mm thick) were isolated as described above from a fourth calf, precultured for 3 days and then cultured for up to 14 days in 0.5 mL of either control medium or control medium supplemented with 20 ng/mL IL-1α. Analysis of mitochondrial activity as an indirect, quantitative measure of viability was performed using the WST-1 assay kit (Biovision, Mountain View, CA) according to the manufacturer's instructions. Briefly, at day 2, 8 or 14, explants ($n = 3$/condition) were incubated with the WST-1 reagent in DMEM for 2 h at 37°C. The conditioned media were then transferred to a 96-well plate and the abundance of formazan product was measured as the absorbance at 450 nm. Viability of one additional explant per group was examined qualitatively by fluorescent staining (Live/Dead®; Invitrogen). Explants were rinsed briefly with DPBS, stained according to the manufacturer's instructions, and bisected along the axial plane. Images of calcein AM (live cells) and ethidium homodimer-1 (dead cells) staining were captured using the appropriate filters on a Zeiss LSM510 confocal microscope with a 20× objective.

MECHANICAL TESTING

Prior to mechanical testing, explants were thawed at room temperature. Thicknesses were measured with digital calipers (Mitutoyo USA, Aurora, IL) and wet masses were determined. Compression testing was performed using a SMT-S 5.6lbf load cell (Interface, Scottsdale, Arizona) and an ELF 3230 testing frame (Enduratec; Minnetonka, MN) at room temperature in 0.15 M DPBS with protease inhibitors, with displacements corrected for load cell compliance. Torsional shear testing was performed using a CVO 120HR stress-controlled rheometer with strain feedback (Bohlin; East Brunswick, NJ).

Samples from the first degradation study were tested in unconfined compression by applying a 0.1 N tare load followed by four steps (5% each, 1 mm/s ramp rate) of stress relaxation with a 10 min relaxation after each strain step. As 10 min may not reflect complete relaxation, the force vs time data $F(t)$ for each step were fit to an analytical solution for the unconfined compression stress relaxation of a linear biphasic material described by Armstrong *et al.*[17]:

$$F(t) = F_\infty \left[1 + \sum_{n=1}^{\infty} A_n \exp\left(-\frac{\alpha_n^2 H_A k t}{a^2}\right)\right],$$

where F_∞ is the equilibrium (relaxed) force, $A_n = 1/[(1-\upsilon)^2\alpha_n^2 - (1-2\upsilon)]$, α_n are the roots to the characteristic Bessel function equation $J_1(x) - (1-\nu)x\, J_o(x)/(1-2\nu) = 0$, a is the sample radius, H_A is the aggregate modulus and k is the permeability. For each relaxation step, a two parameter least squares fit was performed using Matlab 7.1 (Mathworks, Natick, MA) to determine the value of F_∞ and the product $H_A k$, assuming a Poisson's ratio of 0.1 and using the first five terms of the analytical solution. A linear regression of the equilibrium stresses ($F_\infty / \pi a^2$) against the applied strain over the range of 10−20% was used to determine E_{equil}, the unconfined compression equilibrium modulus of each sample.

After relaxation at the second (10%) step, sinusoidal compression (±1.5% strain) was applied at 0.005, 0.05, 0.5, and 5 Hz. For each frequency, the magnitude of the dynamic compressive modulus, $|E^*_{dyn}|$, was calculated by WinTest dynamic mechanical analysis (DMA) software (Enduratec) as the ratio of the fundamental stress and strain magnitudes determined using a Fast Fourier Transform. Samples from the recovery study were similarly tested after a single 10% stress relaxation step to determine the dynamic compressive moduli at 0.01, 0.1, 1.0 and 10 Hz.

Samples from the second degradation study and the recovery study were tested in torsional shear by applying a 10% compressive offset and, after relaxation, applying a nominal 0.5% sinusoidal shear strain at 0.01, 0.1, 1, and 10 Hz. The magnitude of the complex shear modulus $|G^*_{dyn}|$ was determined by the rheometer software from the ratio of the measured stress to the applied strain.

BIOCHEMICAL ANALYSIS

Following mechanical testing, explants were lyophilized overnight and dry masses were determined. Explants were then solubilized with 4 mg/mL proteinase K (Calbiochem) in 100 mM ammonium acetate (pH 6.5) (Sigma). The digested explants and conditioned media were assayed for sGAGs via the dimethylmethylene blue (DMMB) assay[39], using shark chondroitin sulfate (Calbiochem) as a standard. Collagen was assayed via the pDAB/chloramine-T assay for hydroxyproline, using trans-4-hydroxy-L-proline (Sigma) as a standard and assuming a 1:8 mass ratio of hydroxyproline:collagen[40]. As the compressive properties were expected to be related to the matrix fixed charge density (FCD), the sGAG and (for consistency) collagen contents were normalized by water volume in the composition-function analyses.

STATISTICAL ANALYSES

All statistical analyses were performed using Minitab Release 12 (Minitab, Inc., State College, PA) with significance at $p < 0.05$. Collinearity among matrix components or among mechanical properties was determined via linear correlation analyses. Differences among time points in a treatment group or between treatments at a time point were examined via one-way analysis of variance (ANOVA) with Tukey's test for *post hoc* pairwise comparisons. The equilibrium modulus and dynamic shear modulus data were log transformed

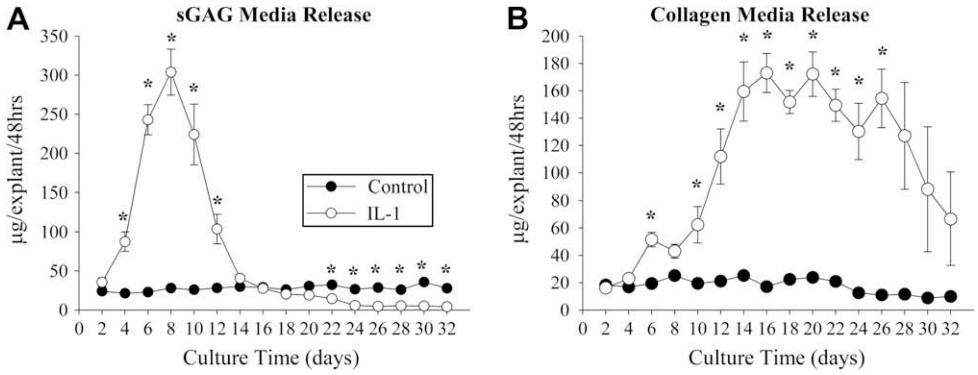

Fig. 1. sGAG (A) and collagen (B) release to the media over 48 h period for control (●) and IL-1-stimulated (○) explants. Data are mean ± SEM. * denotes difference ($p < 0.05$) between control and IL-1-stimulated explants.

prior to ANOVA. Due to loss of sample integrity for IL-1-stimulated explants, sample sizes were insufficient to perform some comparisons at later time points. Regressions of mechanical parameters against matrix constituents were compared between treatment groups as described by Zar[41] using custom Minitab macros. Briefly, the groups were first compared to test the null hypothesis of equal regression slopes. In the case of a common slope, the groups were then compared to test the null hypothesis of equal intercepts. A common regression was used if neither null hypothesis was rejected.

Results

EXPLANT AND MEDIA BIOCHEMISTRY: IL-1 DEGRADATION EXPERIMENTS

As previously demonstrated[14,23,24,26,42,43], treatment with 20 ng/mL IL-1α resulted in substantial matrix depletion over the 32 day culture period. sGAG release for IL-1-stimulated samples peaked at day 8 with 59% of total sGAG released [Fig. 1(A)] and was essentially complete by day 14. Collagen released from IL-1-stimulated explants was significantly elevated over controls at day 6 ($p < 0.05$), peaked near day 14, and persisted through day 24, at which point 74% of total collagen release had occurred [Fig. 1(B)]. Control explants displayed a steady increase in sGAG content, indicating a basal level of PG synthesis [Fig. 2(A)]. The sGAG content of IL-1-stimulated explants decreased during the first 16 days in culture and reached the detection limit of the DMMB assay by day 24. The collagen content of control explants did not vary significantly during the culture period,

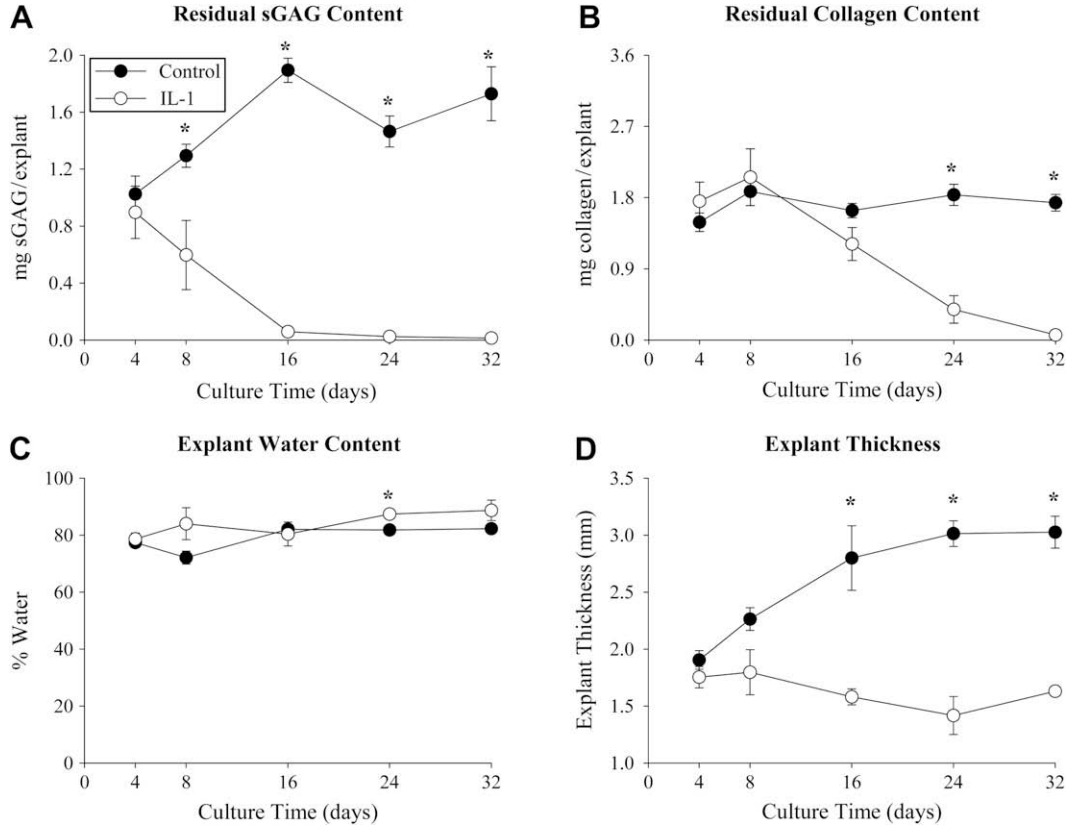

Fig. 2. Residual sGAG content (A), residual collagen content (B), water content (C) and thickness (D) as a function of culture time for control (●) and IL-1-stimulated (○) explants. Data are mean ± SEM. * denotes difference ($p < 0.05$) between control and IL-1-stimulated explants.

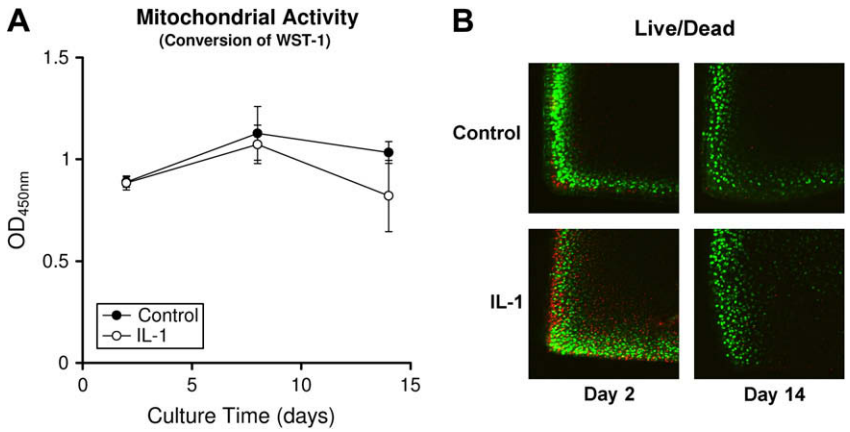

Fig. 3. Mitochondrial activity as measured by conversion of WST-1 (A) and cell viability as indicated by calcein AM (green; live) and ethidium homodimer-1 (red; dead) fluorescence (B) for control (●) and IL-1-stimulated (○) explants.

while the collagen content of the IL-1-stimulated explants gradually decreased following day 8 [Fig. 2(B)]. No differences in cell viability or mitochondrial activity were noted between control and IL-1-stimulated explants [Fig. 3], indicating that cell death did not contribute substantially to the decreases in matrix content with IL-1 exposure. Explant water content showed little variation with culture in either control or IL-1 groups [Fig. 2(C)]. Increases in the thickness of control explants accompanied increases in sGAG [Fig. 2(D)]. In contrast, the thickness of IL-1-stimulated explants did not change significantly during culture.

EXPLANT MECHANICAL PROPERTIES: IL-1 DEGRADATION EXPERIMENTS

The ANOVA indicated a significant effect of time on E_{equil} for controls although no pairwise comparisons were significant [Fig. 4(A)]. $|E^*_{dyn}|$ did not vary significantly during

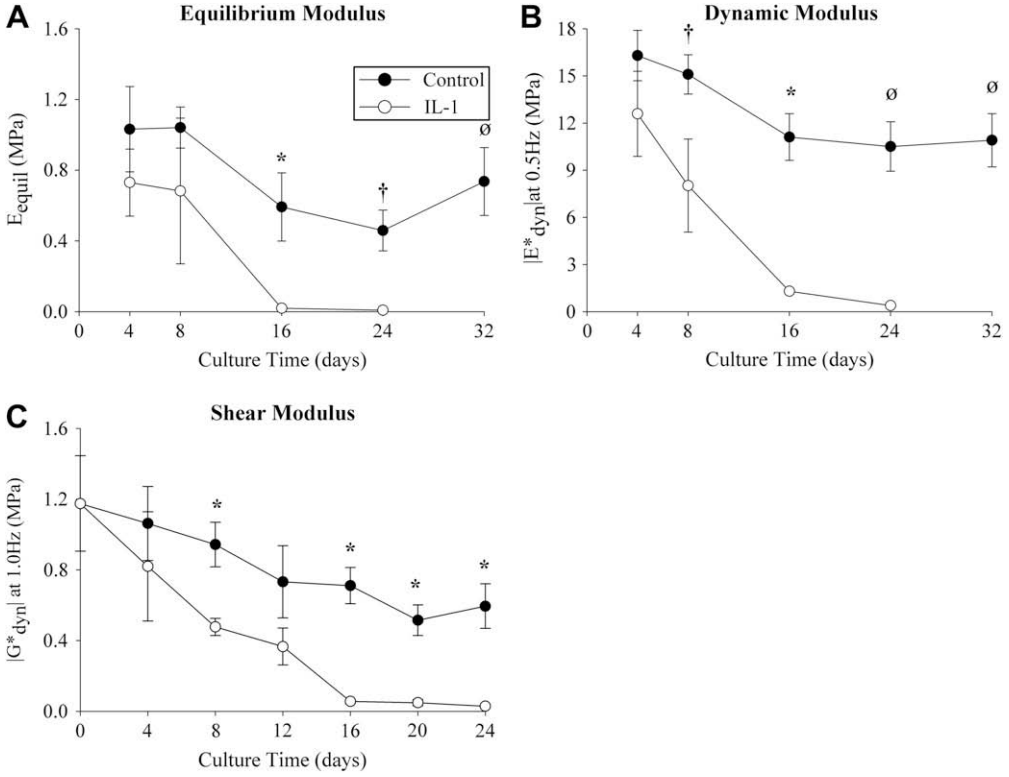

Fig. 4. Compressive and shear properties as a function of culture time for control (●) and IL-1-stimulated (○) explants: (A) Equilibrium unconfined compression modulus; (B) Dynamic unconfined compression modulus at 0.5 Hz; (C) Dynamic shear modulus at 1 Hz. Data are mean ± SEM. * denotes difference ($p < 0.05$) between control and IL-1-stimulated explants. † denotes $p = 0.06$ between control and IL-1-stimulated explants. ∅ denotes an insufficient number of IL-1-stimulated explants to perform the statistical analysis.

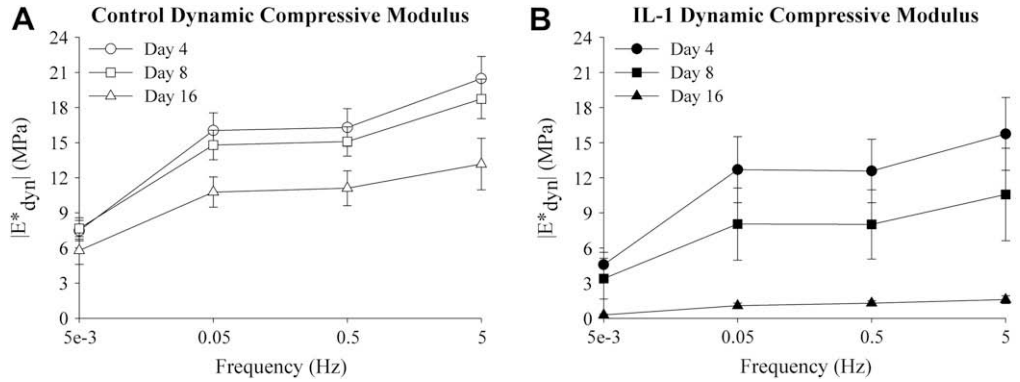

Fig. 5. Dynamic unconfined compression modulus as a function of frequency and culture time for control (A) and IL-1-stimulated (B) explants. Data are mean ± SEM.

culture for control explants [Fig. 4(B)]. In contrast, IL-1-stimulated explants exhibited substantial changes in mechanical properties reflecting the ECM degradation. Both E_{equil} and $|E^*_{dyn}|$ decreased as sGAG was released [Figs. 4(A-B)]. E_{equil} reached detection limits by day 16, whereas $|E^*_{dyn}|$ remained measurable through day 24. IL-1 stimulation for 32 days resulted in sufficient matrix loss that explants could not sustain handling for mechanical testing. $|E^*_{dyn}|$ exhibited similar frequency dependence across time points and treatment groups (Fig. 5).

For control explants, $|G^*_{dyn}|$ remained fairly steady throughout the culture period, as indicated by the non-significant effect of time in the ANOVA (Fig. 4C). In contrast, $|G^*_{dyn}|$ for IL-1-stimulated explants exhibited an initial rapid decrease through day 8 and continued to decrease until it reached detection limits at day 20. As with $|E^*_{dyn}|$, $|G^*_{dyn}|$ exhibited similar frequency dependence across time points and treatment groups (Fig. 6).

EXPLANT AND MEDIA BIOCHEMISTRY: IL-1 RECOVERY EXPERIMENTS

Consistent with the degradation studies, transient IL-1 exposure led to significant early loss of sGAG. Control explants released low levels of sGAG throughout the 20 day culture, whereas substantial amounts of sGAG were released to the culture medium during and immediately following IL-1 stimulation [Fig. 7(A)]. The peak in sGAG release at day 4 coincided with the end of IL-1 exposure. Withdrawal of IL-1 from the culture media was followed by a gradual decrease in sGAG release that reached control levels by day 8. When normalized to account for differences in explant size, the levels of sGAG released are consistent between the degradation and recovery experiments, although a slightly accelerated response to IL-1 occurred in the recovery study. Collagen release was low and comparable in control and IL-1-stimulated explants [Fig. 7(B)], indicating that transient IL-1 exposure did not initiate substantial damage to the collagen network. As in the degradation studies, the sGAG content of control explants gradually increased [Fig. 8(A)]. The IL-1-stimulated explants lost sGAG content over the first 8 days of culture, indicating that the effects of IL-1 exposure persisted beyond the 4 days of stimulation. Between days 8 and 12, explants in the IL-1 group recovered sGAG to the level of the day 4 group, but through day 20 the sGAG content remained significantly below the baseline level of the day 0 group. The collagen content did not vary during culture [Fig. 8(B)]. The water content of control explants did not vary between groups over the first 12 days of culture, but the control group was significantly higher than the IL-1 group at day 20 [Fig. 8(C)]. The difference in water content at day 20 is particularly significant because when the residual sGAG content is normalized by the water content (mL H_2O), there is no difference in sGAG/H_2O at day 20 between control and IL-1 groups (data not shown). The thickness of control explants increased with time, consistent with the accumulation of sGAG, while the thickness of IL-1-stimulated explants did not vary significantly.

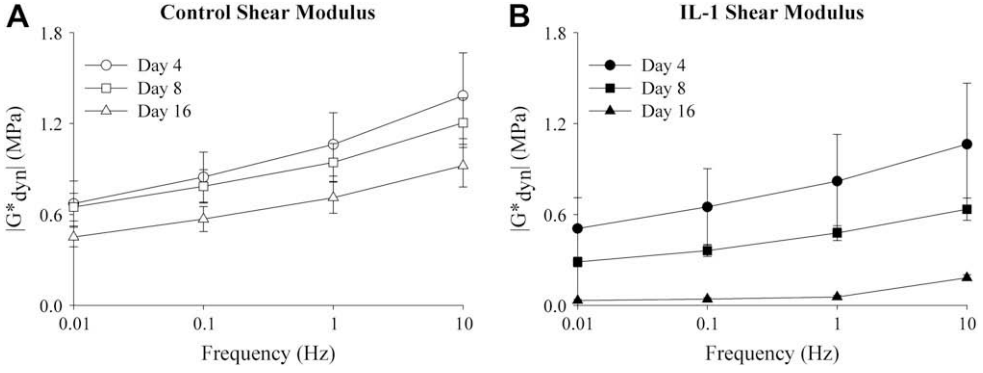

Fig. 6. Dynamic shear modulus as a function of frequency and culture time for control (A) and IL-1-stimulated (B) explants. Data are mean ± SEM.

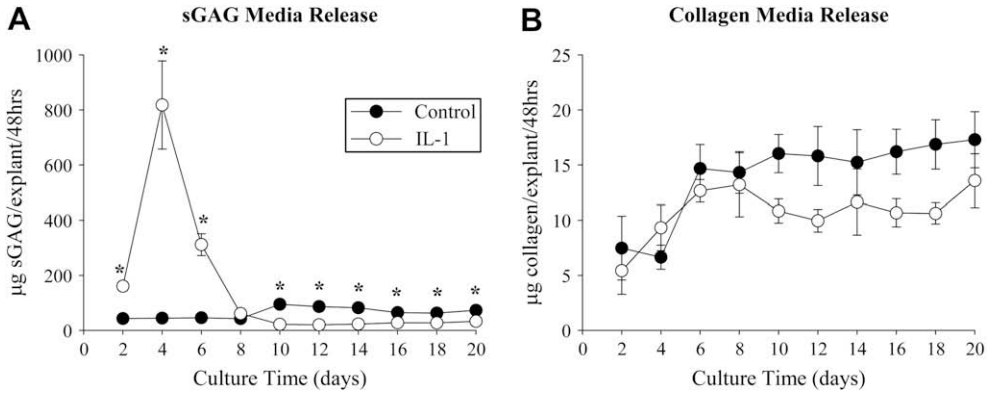

Fig. 7. sGAG (A) and collagen (B) release to the media over 48 h period for control (●) and IL-1-stimulated (○) explants. Data are mean ± SEM. * denotes difference ($p < 0.05$) between control and IL-1-stimulated explants.

EXPLANT MECHANICAL PROPERTIES: IL-1 RECOVERY EXPERIMENTS

Changes in the mechanical properties of explants reflect the observed differences in explant composition. Control explants showed no significant differences in $|E^*_{dyn}|$ or $|G^*_{dyn}|$ with culture [Figs. 9(A-B)]. $|E^*_{dyn}|$ and $|G^*_{dyn}|$ for IL-1-stimulated explants decreased to a minimum at day 8 before recovering to control levels by day 20, despite significantly lower levels of sGAG content. $|E^*_{dyn}|$ and $|G^*_{dyn}|$ exhibited similar frequency dependence across time points and treatment groups (data not shown).

COMPOSITION-FUNCTION RELATIONSHIPS: IL-1 DEGRADATION EXPERIMENTS

Regression analyses indicated substantial differences between control and IL-1-stimulated explants in the dependence of mechanical properties on tissue composition (Table I). The dependence of E_{equil} on sGAG concentration was not significantly different for control and IL-1-stimulated explants, but the regressions were significantly different between treatment groups for all other mechanical properties. The compressive properties of control explants were significantly dependent on sGAG/H_2O [Figs. 10(A-B)] and

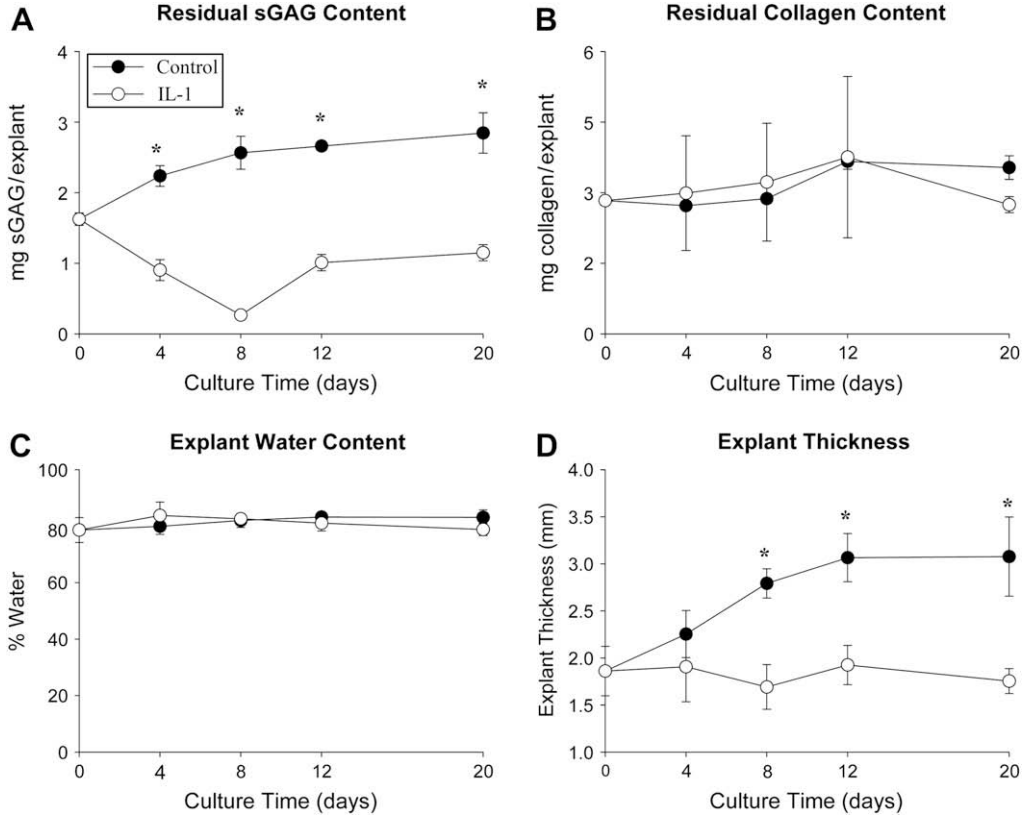

Fig. 8. Residual sGAG content (A), residual collagen content (B), water content (C) and thickness (D) as a function of culture time for control (●) and explants recovering from a 4-day exposure to IL-1 (○). Data are mean ± SEM. * denotes difference ($p < 0.05$) between control and IL-1-stimulated explants.

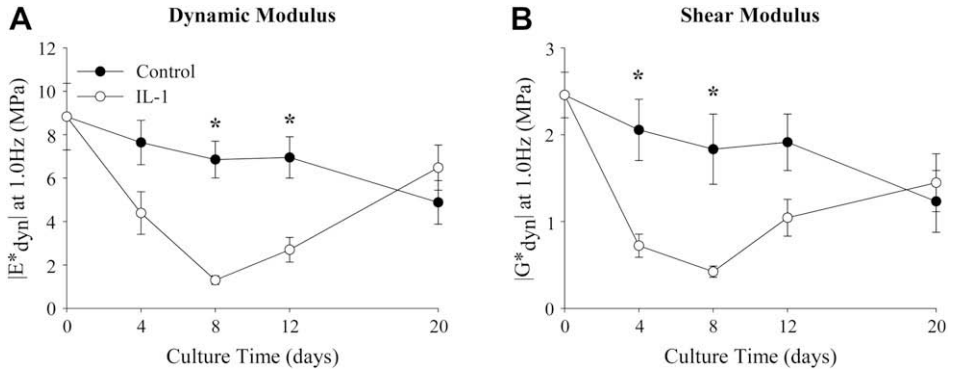

Fig. 9. Dynamic unconfined compression modulus at 1.0 Hz (A) and dynamic shear modulus at 1.0 Hz (B) as functions of culture time for control (●) explants and explants following a 4-day transient exposure to IL-1 (○). Data are mean ± SEM. * denotes difference ($p < 0.05$) between control and IL-1-stimulated explants.

collagen/H_2O [Figs. 10(D-E)]. In contrast, for IL-1-stimulated explants, all compressive properties were strongly dependent on sGAG/H_2O [Figs. 10(A-B)] but exhibited no dependence on collagen/H_2O [Figs. 10(D-E)]. Both for control and IL-1-stimulated explants, $|G^*_{dyn}|$ was strongly dependent on sGAG/H_2O [Fig. 10(C)] and weakly dependent on collagen/H_2O [Fig. 10(F)]. Regression results of $|E^*_{dyn}|$ and $|G^*_{dyn}|$ at 0.5 Hz and 1.0 Hz, respectively, were consistent with analysis at all frequencies tested.

Collinearities among ECM components and among the measured mechanical properties were examined to aid in interpreting the composition-function regression analyses. Data from all time points were pooled for control and IL-1-stimulated explants. Significant, negative correlations were found between percent water and both collagen and sGAG concentrations for control and IL-1 groups (Table II). A significant, positive correlation was found between collagen and sGAG concentrations for control explants but not for IL-1-stimulated explants, reflecting the decoupled sGAG and collagen release profiles. Significant, positive correlation coefficients were found among all compressive mechanical properties for both the control and IL-1 groups (Table III). In control and IL-1-stimulated explants, high correlations ($0.877 < R < 0.929$) were found between $|E_{equil}|$ and $|E^*_{dyn}|$, suggesting that the measurements offer similar predictions of the mechanical integrity of the ECM. Regressions of $|E^*_{dyn}|$ at 0.5 Hz and $|G^*_{dyn}|$ at 1.0 Hz were consistent at the other tested frequencies.

COMPOSITION-FUNCTION RELATIONSHIPS: IL-1 RECOVERY EXPERIMENTS

Consistent with the IL-1 degradation studies, regression analysis of the IL-1 recovery data indicated the differential dependence of mechanical properties on matrix composition (Fig. 11, Table IV). No dependence on collagen content was found for IL-1-stimulated explants for either $|E^*_{dyn}|$ or $|G^*_{dyn}|$, reflecting the stable collagen contents. The depletion and subsequent recovery of sGAG in the IL-1 group was reflected in a strong dependence of $|E^*_{dyn}|$ and $|G^*_{dyn}|$ on sGAG/H_2O. For control explants, sGAG/H_2O and collagen//H_2O were significant predictors of $|G^*_{dyn}|$ but not of $|E^*_{dyn}|$.

Discussion

The relationships between articular cartilage matrix composition and tissue mechanical properties were investigated in immature bovine explants during exhaustive IL-1-induced degradation and during transient IL-1 exposure and recovery. Detailed time courses of the biochemical and biophysical changes associated with persistent and transient proinflammatory stimulation were generated in a common model for studying cartilage matrix catabolism, and regression analyses revealed similar composition-function relationships in degrading and recovering cartilage. Significantly, $|E^*_{dyn}|$ and $|G^*_{dyn}|$ for the transiently

Table I
Linear regressions of physical properties against biochemical composition for IL-1 degradation study

y		$y = a \times x + b$					
		$x =$ sGAG/H_2O (mg/mL)			$x =$ collagen/H_2O (mg/mL)		
		r^2	a	b	r^2	a	b
E_{equil}	Control	0.66	9.03E-03	−5.76E-02	0.48	6.19E-03	5.54E-03
	IL-1-stimulated				NS	–	–
$\|E^*_{dyn}\|$	Control	0.27	6.88E-02	6.47E+00	0.51	5.77E-02	6.03E+00
	IL-1-stimulated	0.96	1.53E-01	−3.12E-01	NS	–	–
$\|G^*_{dyn}\|$	Control	0.53	1.874E+04	−2.77E+05	0.26	4.15E+03	3.76E+05
	IL-1-stimulated			1.28E+05			−2.49E+

Linear regression coefficients are significant at $p < 0.05$ (NS = non-significant). Common regression coefficients are indicated by a numerical value that spans the two groups. (E_{equil} = Equilibrium Unconfined Compression Modulus; $|E^*_{dyn}|$ = Magnitude of Dynamic Compression Modulus at 0.5 Hz; $|G^*_{dyn}|$ = Magnitude of Dynamic Shear Modulus at 1 Hz; Units of all mechanical properties are in MPa).

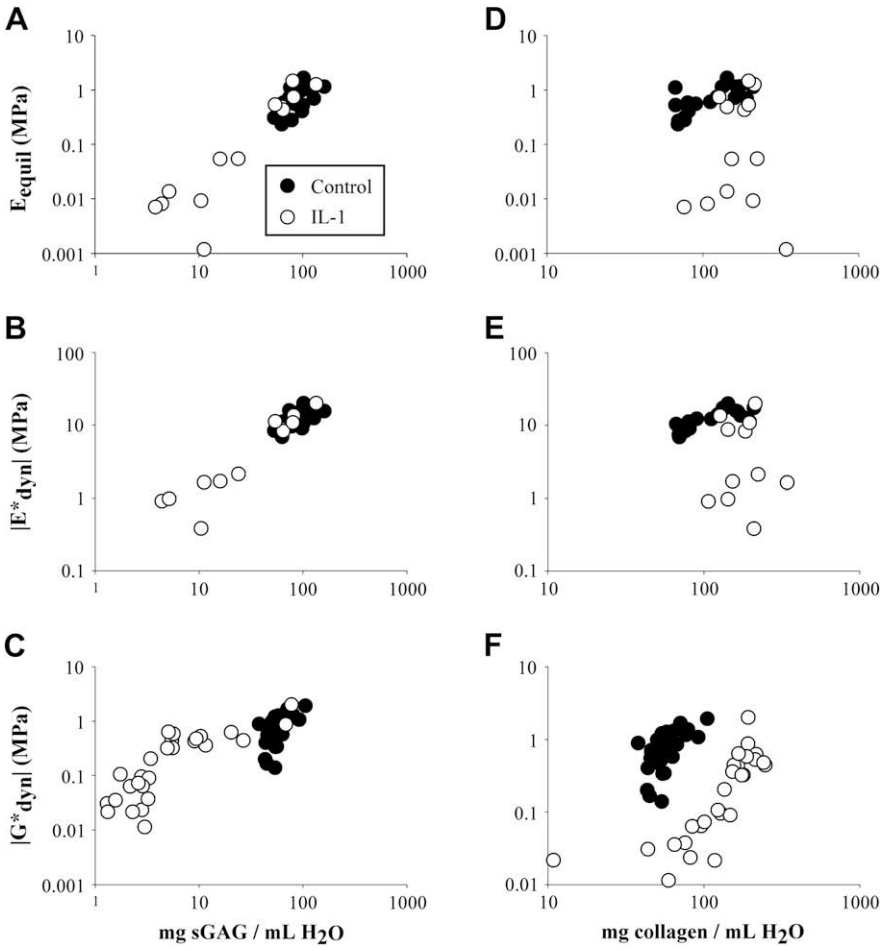

Fig. 10. Physical properties plotted against sGAG concentration (A–C) and collagen concentration (D–F) for control (●) and IL-1-stimulated (○) explants. Note that data are presented on logarithmic scales.

stimulated IL-1 explants recovered to levels similar to control explants despite incomplete repopulation of the matrix with sGAG. The mechanical properties of untreated explants were generally dependent on both sGAG and collagen concentration, which is consistent with previous reports[2,4,6,20,45,46]. The physical properties of cartilage continuously and transiently stimulated with IL-1 were strongly dependent on sGAG content, with only the shear modulus of continuously stimulated cartilage significantly related to collagen content. These results underscore the importance of sGAG concentration in the maintenance of tissue mechanical function and lend support to therapeutic strategies aimed at promoting sGAG synthesis and diagnostic approaches to monitor degradation and recovery by tracking changes in sGAG/H_2O.

The concurrent loss of sGAG and mechanical properties following IL-1 stimulation likely accounts for the strong correlation between cartilage sGAG concentration and mechanical properties. Further, it is not surprising that the mechanical properties exhibited minimal dependence on collagen content, since the loss of biomechanical function preceded significant collagen depletion in these experiments. Likewise, the recovery of explant mechanical properties following transient IL-1 exposure correlated well with increases in sGAG and water content while there was no change in collagen content. Direct enzymatic

Table II
Correlations between biochemical constituents for control and IL-1-stimulated cartilage explants

	Control		IL-1-stimulated	
	Collagen/H_2O	sGAG/H_2O	Collagen/H_2O	sGAG/H_2O
sGAG/H_2O	+0.780		NS	
% H_2O	−0.915	−0.687	−0.775	−0.630

Correlation coefficients are significant at $p < 0.05$ (NS = non-significant).

Table III
Correlations between compressive properties of control and IL-1-stimulated explants

$p < 0.05$	Control	IL-1-stimulated
	E_{equil}	E_{equil}
$\|E^*_{dyn}\|$	+0.929	+0.877

Correlation coefficients are significant at $p < 0.05$. (E_{equil} = Equilibrium Unconfined Compression Modulus; $|E^*_{dyn}|$ = Magnitude of Dynamic Compression Modulus at 0.5 Hz).

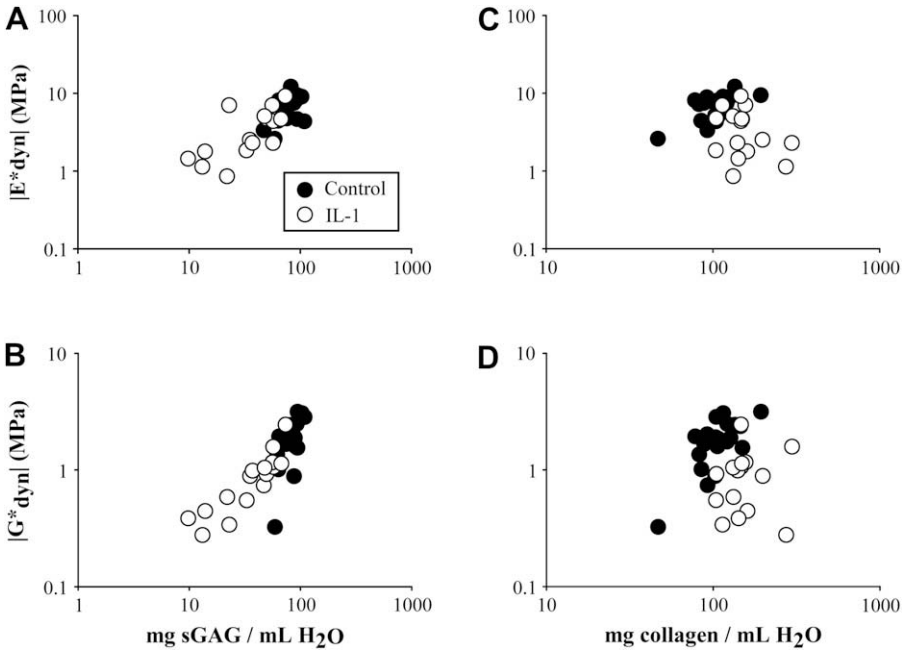

Fig. 11. Physical properties plotted against sGAG concentration (A-B) and collagen concentration (C-D) for control (●) and IL-1-stimulated (○) explants. Note that data are presented on logarithmic scales.

digestion of collagen with collagenases has been used to investigate the specific dependence of mechanical properties on collagen[46], but the results of this model are difficult to interpret given the nonspecific activity of collagenases on aggrecan[47–49] and any role of the collagen network in retaining PG aggregates. The results presented here highlight the functional implications of sGAG depletion in the early stages of cytokine-induced cartilage degradation, but due to the experimental model yield little direct insight into the dependence on collagen content in normal or degraded cartilage.

Previous studies have described the loss of ECM and mechanical properties during persistent IL-1 stimulation of cartilage explants[14,23,24,26,42–44], and PG content has been restored in cartilage explants following IL-1 insult *in vitro* and *in vivo*[34–37,50]. The results of this study demonstrate the chondrocyte's potential (albeit under *in vitro* culture conditions) to reestablish the tissue's mechanical function following partial matrix degradation and indicate that functional recovery of $|E^*_{dyn}|$ and $|G^*_{dyn}|$ can be achieved with incomplete repopulation of sGAG content. Recovered explants contained 40% of the sGAG of the control explants after 16 days of recovery (day 20) and equal levels of collagen content, yet $|E^*_{dyn}|$ and $|G^*_{dyn}|$ were not statistically different from those of the control explants. However, when sGAG concentration was calculated from the explant water content (to approximate FCD), no difference was noted between control and IL-1-stimulated explants at day 20. This finding demonstrates the utility of FCD (approximated by sGAG concentration) as an indicator of cartilage health and function.

Given the complex ECM organization and nonlinear mechanical behavior of articular cartilage, the linear regression analyses used here may not capture the true composition-function relationships. Indeed, Donnan and Poisson–Boltzmann models[51,52] predict that osmotic swelling is a nonlinear function of PG concentration. The correlations described here may also be biased by the range of PGs and collagen content examined, particularly given the heteroscedasticity over a wide range of matrix density. The composition-function relationships may be further influenced by the choice of biochemical parameters (i.e., collagen, sGAG, water). Other studies describing composition-function relationships have included collagen cleavage

Table IV
Linear regressions of physical properties against biochemical composition for IL-1 recovery study

y		$y = a \times x + b$					
		$x = \text{sGAG/H}_2\text{O}$ (mg/mL)			$x = \text{collagen/H}_2\text{O}$ (mg/mL)		
		r^2	*a*	*b*	r^2	*a*	*b*
$\|E^*_{dyn}\|$	Control	NS	–	–	NS	–	–
	IL-1-stimulated	0.61	9.88E-02	−1.07E-01	NS	–	–
$\|G^*_{dyn}\|$	Control	0.43	3.36E-02	−8.29E-01	0.42	1.48E-02	2.55E-01
	IL-1-stimulated	0.83	2.91E-02	−2.10E-01	NS	–	–

Linear regression coefficients are significant at $p < 0.05$ (NS = non-significant). Common regression coefficients are indicated by a numerical value that spans the two groups. ($|E^*_{dyn}|$ = Magnitude of Dynamic Compression Modulus at 1 Hz; $|G^*_{dyn}|$ = Magnitude of Dynamic Shear Modulus at 1 Hz; Units of all mechanical properties are in MPa).

products[15] and collagen crosslinks as ECM components[6,7,15,53]. Collagen crosslinks and cleavage products may be critical parameters to examine since the integrity of the collagen network cannot be evaluated by the hydroxyproline assay used in the present study. Despite the additional parameters and models that could be used to analyze the data, the significance and strength of the correlations reported here demonstrate the fundamental importance of sGAG to the compressive and shear properties of articular cartilage.

The composition-function relationships observed in untreated and IL-1-stimulated immature bovine cartilage may be specific to this tissue's age, species, and anatomic origin. Mature articular cartilage contains a significantly higher collagen fiber and collagen crosslink density[6,54], lower PG content[54], shorter sGAG chain length[55–58], and fewer cells[59] than immature cartilage. IL-1-induced matrix degradation may be more aggressive in immature than mature cartilage due to the higher cell density, although the sensitivity of human articular cartilage to IL-1 stimulation appears to be independent of age[60]. Variations in articular cartilage ECM composition and mechanical properties have also been reported with tissue depth[61,62] and topographical location[7,45]. While the present study did not examine variations in composition-function relationships with topographical location, the use of immature middle zone cartilage minimizes variations due to tissue inhomogeneity through the tissue depth.

The strong dependence of all measured physical properties on sGAG concentration during IL-1-induced degeneration but prior to the onset of major collagen depletion suggests that measurements of sGAG concentration may be a useful surrogate for direct mechanical measurements in early stage degeneration. For example, imaging techniques such as delayed gadolinium-enhanced MRI of cartilage (dGEMRIC)[63] and EPIC-μCT (Equilibrium Partitioning of an Ionic Contrast agent via microcomputed tomography)[64] produce maps of tissue FCD that may provide sufficient information to noninvasively estimate the mechanical properties of injured or diseased cartilage *in vivo*. The application of composition-function relationships with these quantitative imaging techniques may also have utility in evaluating the competency of engineered cartilage grafts and resurfaced joints.

Conflict of interest

The authors have no conflicts of interest to disclose.

Acknowledgements

We thank Dr Elsie Eugui and Dr Fengrong Zuo for helpful conversations regarding these studies. This work was funded by an Arthritis Foundation Arthritis Investigator grant, the ERC program of the NSF under award number EEC-9731643 (Georgia Tech/Emory Center (GTEC) for the Engineering of Living Tissues), a graduate fellowship under NSF IGERT award number 0221600 (AWP), a graduate fellowship from the Cellular and Tissue Engineering Training Grant Program under NIH award number 5 T32 GM008433-13 (CGW), and by Roche Palo Alto. The study sponsors were not involved in the study design or execution or in the manuscript preparation.

Sources of Support: Arthritis Foundation Arthritis Investigator grant, the ERC program of the NSF under award number EEC-9731643 (Georgia Tech/Emory Center (GTEC) for the Engineering of Living Tissues), a graduate fellowship under NSF IGERT award number 0221600 (AWP), a graduate fellowship from the Cellular and Tissue Engineering Training Grant Program under NIH award number 5 T32 GM008433-13 (CGW), by Roche Palo Alto.

References

1. Park S, Krishnan R, Nicoll SB, Ateshian GA. Cartilage interstitial fluid load support in unconfined compression. J Biomech. Dec 2003; 36(12):1785–96.
2. Mow VC, Ratcliffe A. Structure and function of articular cartilage and meniscus. In: Mow VC, Hayes WC, Eds. Basic Orthopaedic Biomechanics. 2nd edn. Philadelphia: Lippincott-Raven; 1997:113–77.
3. Poole AR, Kojima T, Yasuda T, Mwale F, Kobayashi M, Laverty S. Composition and structure of articular cartilage: a template for tissue repair. Clin Orthop. Oct 2001;(391 Suppl):S26–33.
4. Basser PJ, Schneiderman R, Bank RA, Wachtel E, Maroudas A. Mechanical properties of the collagen network in human articular cartilage as measured by osmotic stress technique. Arch Biochem Biophys Mar 15 1998;351(2):207–19.
5. Kuettner KE. Biochemistry of articular cartilage in health and disease. Clin Biochem Jun 1992;25(3):155–63.
6. Williamson AK, Chen AC, Sah RL. Compressive properties and function-composition relationships of developing bovine articular cartilage. J Orthop Res Nov 2001;19(6):1113–21.
7. Williamson AK, Chen AC, Masuda K, Thonar EJ, Sah RL. Tensile mechanical properties of bovine articular cartilage: variations with growth and relationships to collagen network components. J Orthop Res Sep 2003;21(5):872–80.
8. Williamson AK, Masuda K, Thonar EJ, Sah RL. Growth of immature articular cartilage *in vitro*: correlated variation in tensile biomechanical and collagen network properties. Tissue Eng Aug 2003;9(4):625–34.
9. Vunjak-Novakovic G, Martin I, Obradovic B, Treppo S, Grodzinsky AJ, Langer R, *et al.* Bioreactor cultivation conditions modulate the composition and mechanical properties of tissue-engineered cartilage. J Orthop Res Jan 1999;17(1):130–8.
10. Setton LA, Mow VC, Muller FJ, Pita JC, Howell DS. Altered structure-function relationships for articular cartilage in human osteoarthritis and an experimental canine model. Agents Actions Suppl 1993;39:27–48.
11. Rivers PA, Rosenwasser MP, Mow VC, Pawluk RJ, Strauch RJ, Sugalski MT, *et al.* Osteoarthritic changes in the biochemical composition of thumb carpometacarpal joint cartilage and correlation with biomechanical properties. J Hand Surg [Am] Sep 2000;25(5): 889–98.
12. Kempson GE, Muir H, Pollard C, Tuke M. The tensile properties of the cartilage of human femoral condyles related to the content of collagen and glycosaminoglycans. Biochim Biophys Acta Feb 28 1973;297(2): 456–72.
13. Kelly DJ, Crawford A, Dickinson SC, Sims TJ, Mundy J, Hollander AP, *et al.* Biochemical markers of the mechanical quality of engineered hyaline cartilage. J Mater Sci Mater Med Feb 2007;18(2):273–81.
14. Bonassar LJ, Sandy JD, Lark MW, Plaas AH, Frank EH, Grodzinsky AJ. Inhibition of cartilage degradation and changes in physical properties induced by IL-1 beta and retinoic acid using matrix metalloproteinase inhibitors. Arch Biochem Biophys Aug 15 1997;344(2):404–12.
15. Bank RA, Soudry M, Maroudas A, Mizrahi J, TeKoppele JM. The increased swelling and instantaneous deformation of osteoarthritic cartilage is highly correlated with collagen degradation. Arthritis Rheum Oct 2000;43(10):2202–10.
16. Narmoneva DA, Wang JY, Setton LA. A noncontacting method for material property determination for articular cartilage from osmotic loading. Biophys J Dec 2001;81(6):3066–76.
17. Armstrong CG, Lai WM, Mow VC. An analysis of the unconfined compression of articular cartilage. J Biomech Eng May 1984;106(2):165–73.
18. Park S, Hung CT, Ateshian GA. Mechanical response of bovine articular cartilage under dynamic unconfined compression loading at physiological stress levels. Osteoarthritis Cartilage Jan 2004;12(1):65–73.
19. Laasanen MS, Toyras J, Korhonen RK, Rieppo J, Saarakkala S, Nieminen MT, *et al.* Biomechanical properties of knee articular cartilage. Biorheology 2003;40(1-3):133–40.
20. Zhu W, Mow VC, Koob TJ, Eyre DR. Viscoelastic shear properties of articular cartilage and the effects of glycosidase treatments. J Orthop Res Nov 1993;11(6):771–81.
21. Korhonen RK, Laasanen MS, Toyras J, Rieppo J, Hirvonen J, Helminen HJ, *et al.* Comparison of the equilibrium response of articular cartilage in unconfined compression, confined compression and indentation. J Biomech Jul 2002;35(7):903–9.
22. Lu XL, Sun DD, Guo XE, Chen FH, Lai WM, Mow VC. Indentation determined mechanoelectrochemical properties and fixed charge density of articular cartilage. Ann Biomed Eng Mar 2004;32(3):370–9.

23. Arner EC, Hughes CE, Decicco CP, Caterson B, Tortorella MD. Cytokine-induced cartilage proteoglycan degradation is mediated by aggrecanase. Osteoarthritis Cartilage May 1998;6:214–28.
24. Legare A, Garon M, Guardo R, Savard P, Poole AR, Buschmann MD. Detection and analysis of cartilage degeneration by spatially resolved streaming potentials. J Orthop Res Jul 2002;20(4):819–26.
25. Karsdal MA, Madsen SH, Christiansen C, Henriksen K, Fosang AJ, Sondergaard BC. Cartilage degradation is fully reversible in the presence of aggrecanase but not matrix metalloproteinase activity. Arthritis Res Ther 2008;10(3):R63.
26. Kozaci LD, Buttle DJ, Hollander AP. Degradation of type II collagen, but not proteoglycan, correlates with matrix metalloproteinase activity in cartilage explant cultures. Arthritis Rheum Jan 1997;40(1):164–74.
27. Arner EC, Pratta MA. Independent effects of interleukin-1 on proteoglycan breakdown, proteoglycan synthesis, and prostaglandin E2 release from cartilage in organ culture. Arthritis Rheum Mar 1989; 32(3):288–97.
28. Smith RJ, Rohloff NA, Sam LM, Justen JM, Deibel MR, Cornette JC. Recombinant human interleukin-1 alpha and recombinant human interleukin-1 beta stimulate cartilage matrix degradation and inhibit glycosaminoglycan synthesis. Inflammation Aug 1989;13(4):367–82.
29. Neidel J, Zeidler U. Independent effects of interleukin 1 on proteoglycan synthesis and proteoglycan breakdown of bovine articular cartilage *in vitro*. Agents Actions May 1993;39(1-2):82–90.
30. Tyler JA, Benton HP. Synthesis of type II collagen is decreased in cartilage cultured with interleukin 1 while the rate of intracellular degradation remains unchanged. Coll Relat Res Sep 1988;8(5):393–405.
31. Goldring MB. Control of collagen synthesis in human chondrocyte cultures by immune interferon and interleukin-1. J Rheumatol May 1987;64–6. 14 Spec No.
32. Goldring MB, Krane SM. Modulation by recombinant interleukin 1 of synthesis of types I and III collagens and associated procollagen mRNA levels in cultured human cells. J Biol Chem Dec 5 1987;262(34):16724–9.
33. Wang J, Verdonk P, Elewaut D, Veys EM, Verbruggen G. Homeostasis of the extracellular matrix of normal and osteoarthritic human articular cartilage chondrocytes *in vitro*. Osteoarthritis Cartilage Nov 2003; 11(11):801–9.
34. Williams A, Oppenheimer RA, Gray ML, Burstein D. Differential recovery of glycosaminoglycan after IL-1-induced degradation of bovine articular cartilage depends on degree of degradation. Arthritis Res Ther 2003;5(2):R97–105.
35. Rayan V, Hardingham T. The recovery of articular cartilage in explant culture from interleukin-1 alpha: effects on proteoglycan synthesis and degradation. Matrix Biol Apr 1994;14(3):263–71.
36. van de Loo AA, Arntz OJ, Otterness IG, van den Berg WB. Proteoglycan loss and subsequent replenishment in articular cartilage after a mild arthritic insult by IL-1 in mice: impaired proteoglycan turnover in the recovery phase. Agents Actions May 1994;41(3-4):200–8.
37. Page Thomas DP, King B, Stephens T, Dingle JT. In vivo studies of cartilage regeneration after damage induced by catabolin/interleukin-1. Ann Rheum Dis Feb 1991;50(2):75–80.
38. Pratta MA, Yao W, Decicco C, Tortorella MD, Liu RQ, Copeland RA, *et al*. Aggrecan protects cartilage collagen from proteolytic cleavage. J Biol Chem Nov 14 2003;278(46):45539–45.
39. Farndale RW, Sayers CA, Barrett AJ. A direct spectrophotometric microassay for sulfated glycosaminoglycans in cartilage cultures. Connect Tissue Res 1982;9(4):247–8.
40. Woessner Jr JF. The determination of hydroxyproline in tissue and protein samples containing small proportions of this imino acid. Arch Biochem Biophys May 1961;93:440–7.
41. Zar JH. Biostatistical Analysis. 2nd edn. Englewood Cliffs, NJ: Prentice Hall; 1984
42. Billinghurst RC, Wu W, Ionescu M, Reiner A, Dahlberg L, Chen J, *et al*. Comparison of the degradation of type II collagen and proteoglycan in nasal and articular cartilages induced by interleukin-1 and the selective inhibition of type II collagen cleavage by collagenase. Arthritis Rheum Mar 2000;43(3):664–72.
43. Stabellini G, De Mattei M, Calastrini C, Gagliano N, Moscheni C, Pasello M, *et al*. Effects of interleukin-1beta on chondroblast viability and extracellular matrix changes in bovine articular cartilage explants. Biomed Pharmacother Sep 2003;57(7):314–9.
44. Wilson CG, Palmer AW, Zuo F, Eugui E, Wilson S, Mackenzie R, *et al*. Selective and non-selective metalloproteinase inhibitors reduce IL-1-induced cartilage degradation and loss of mechanical properties. Matrix Biol May 2007;26(4):259–68.
45. Treppo S, Koepp H, Quan EC, Cole AA, Kuettner KE, Grodzinsky AJ. Comparison of biomechanical and biochemical properties of cartilage from human knee and ankle pairs. J Orthop Res Sep 2000;18(5):739–48.
46. Rieppo J, Toyras J, Nieminen MT, Kovanen V, Hyttinen MM, Korhonen RK, *et al*. Structure-function relationships in enzymatically modified articular cartilage. Cells Tissues Organs 2003;175(3): 121–32.
47. Fosang AJ, Last K, Knauper V, Neame PJ, Murphy G, Hardingham TE, *et al*. Fibroblast and neutrophil collagenases cleave at two sites in the cartilage aggrecan interglobular domain. Biochem J Oct 1 1993; 295(Pt 1):273–6.
48. Arner EC, Decicco CP, Cherney R, Tortorella MD. Cleavage of native cartilage aggrecan by neutrophil collagenase (MMP-8) is distinct from endogenous cleavage by aggrecanase. J Biol Chem Apr 4 1997;272(14):9294–9.
49. Fosang AJ, Last K, Knauper V, Murphy G, Neame PJ. Degradation of cartilage aggrecan by collagenase-3 (MMP-13). FEBS Lett Feb 12 1996;380(1-2):17–20.
50. Homandberg GA, Ummadi V, Kang H. High molecular weight hyaluronan promotes repair of IL-1 beta-damaged cartilage explants from both young and old bovines. Osteoarthritis Cartilage Mar 2003; 11(3):177–86.
51. Buschmann MD, Grodzinsky AJ. A molecular model of proteoglycan-associated electrostatic forces in cartilage mechanics. J Biomech Eng May 1995;117(2):179–92.
52. Maroudas A. Physio-chemical properties of articular cartilage. In: Freeman MAR, Ed. Adult Articular Cartilage. 2nd edn. Tunbridge Wells, England: Pitman; 1979:215–90.
53. Guilak F, Meyer BC, Ratcliffe A, Mow VC. The effects of matrix compression on proteoglycan metabolism in articular cartilage explants. Osteoarthritis Cartilage Jun 1994;2(2):91–101.
54. Brama PA, Tekoppele JM, Bank RA, Barneveld A, van Weeren PR. Functional adaptation of equine articular cartilage: the formation of regional biochemical characteristics up to age one year. Equine Vet J May 2000;32(3):217–21.
55. Front P, Aprile F, Mitrovic DR, Swann DA. Age-related changes in the synthesis of matrix macromolecules by bovine articular cartilage. Connect Tissue Res 1989;19(2-4):121–33.
56. Brown MP, West LA, Merritt KA, Plaas AH. Changes in sulfation patterns of chondroitin sulfate in equine articular cartilage and synovial fluid in response to aging and osteoarthritis. Am J Vet Res Jun 1998;59(6): 786–91.
57. Bayliss MT, Osborne D, Woodhouse S, Davidson C. Sulfation of chondroitin sulfate in human articular cartilage. The effect of age, topographical position, and zone of cartilage on tissue composition. J Biol Chem May 28 1999;274(22):15892–900.
58. Ng L, Grodzinsky AJ, Patwari P, Sandy J, Plaas A, Ortiz C. Individual cartilage aggrecan macromolecules and their constituent glycosaminoglycans visualized via atomic force microscopy. J Struct Biol Sep 2003;143(3):242–57.
59. Jadin KD, Wong BL, Bae WC, Li KW, Williamson AK, Schumacher BL, *et al*. Depth-varying density and organization of chondrocytes in immature and mature bovine articular cartilage assessed by 3D imaging and analysis. J Histochem Cytochem Sep 2005;53(9):1109–19.
60. Hickery MS, Bayliss MT, Dudhia J, Lewthwaite JC, Edwards JC, Pitsillides AA. Age-related changes in the response of human articular cartilage to IL-1alpha and transforming growth factor-beta (TGF-beta): chondrocytes exhibit a diminished sensitivity to TGF-beta. J Biol Chem Dec 26 2003;278(52):53063–71.
61. Schinagl RM, Gurskis D, Chen AC, Sah RL. Depth-dependent confined compression modulus of full-thickness bovine articular cartilage. J Orthop Res Jul 1997;15(4):499–506.
62. Chen AC, Bae WC, Schinagl RM, Sah RL. Depth- and strain-dependent mechanical and electromechanical properties of full-thickness bovine articular cartilage in confined compression. J Biomech Jan 2001; 34(1):1–12.
63. Samosky JT, Burstein D, Eric Grimson W, Howe R, Martin S, Gray ML. Spatially-localized correlation of dGEMRIC-measured GAG distribution and mechanical stiffness in the human tibial plateau. J Orthop Res Jan 2005;23(1):93–101.
64. Palmer AW, Guldberg RE, Levenston ME. Analysis of cartilage matrix fixed charge density and three-dimensional morphology via contrast-enhanced microcomputed tomography. Proc Natl Acad Sci U S A Dec 19 2006;103(51):19255–60.